Conf-940809--1

LA-UR-93- 93-2435
N-6-93-R118

Los Alamos National Laboratory is operated by the University of California for the United States Department of Energy under contract W-7405-ENG-36

TITLE: UNIFYING THE CONTROLLING MECHANISMS FOR THE CRITICAL HEAT FLUX AND QUENCHING: THE ABILITY OF LIQUID TO CONTACT THE HOT SURFACE

PART III: THE INFLUENCE OF DRY-PATCH SHAPE AND MULTIPLE-PATCH INTERACTION

AUTHOR(S): Cetin Unal
Pratap Sadasivan
Ralph A. Nelson

SUBMITTED TO: 10th International Heat Transfer Conference
August 14, 1994
Brighton, England

DISCLAIMER

MASTER

Los Alamos
Los Alamos National Laboratory
Los Alamos, New Mexico 87545

DISCLAIMER

Portions of this document may be illegible in electronic image products. Images are produced from the best available original document.

UNIFYING THE CONTROLLING MECHANISMS FOR THE CRITICAL HEAT FLUX AND QUENCHING: THE ABILITY OF LIQUID TO CONTACT THE HOT SURFACE

PART III: THE INFLUENCE OF DRY-PATCH SHAPE AND MULTIPLE-PATCH INTERACTION

by

Cetin Unal, Pratap Sadasivan, and Ralph A. Nelson

Los Alamos National Laboratory
Nuclear Technology and Engineering Division
Engineering and Safety Analysis Group
Los Alamos, NM 87545

ABSTRACT

In earlier work, we proposed a hypothesis for the occurrence of critical heat flux (CHF) during pool boiling of saturated liquids. According to this hypothesis, CHF occurs when some portion of the heater surface dries and a local point within this dry patch reaches a critical rewetting temperature, beyond which liquid can no longer contact that point. In this paper, the effects of dry-patch shape and multiple-patch interactions on the critical rewetting temperature have been investigated.

The study revealed the effect of the noncircular shape of the dry patch on the calculated rewetting temperatures to be negligible. In the case of a single dry patch, the location of the patch on the heater surface had also a negligible effect on the rewetting

temperature. The spatial distribution of multiple dry patches on the heater surface did not affect the rewetting temperature significantly. The number of patches, however, did affect the rewetting temperature. Its effect was found to be of the same order as that of the initial thickness reported in the previous study (Unal et al. 1991).

Results reveal that the predominant influences in the calculation of the rewetting temperature are the initial macrolayer thickness and the number of patches. Because the number of patches is ultimately related to the spatial distribution of the initial macrolayer thickness over the heater surface, this further underscores the fact that an accurate treatment of the dry-patch behavior and its role in the mechanism of CHF must include appropriate consideration of the spatial variation in the macrolayer thickness over the heater surface. Therefore, although a two-dimensional, axial-symmetric model would be sufficient from the point of view of dry-patch shape and its spatial distribution, a three-dimensional model is needed for proper consideration of the spatial variation in the macrolayer thickness and the number of patches.

NOMENCLATURE

A	Area
a	Semiminor axis of ellipse
b	Semimajor axis of ellipse
C_p	Specific heat
f	Constant
h	Heat-transfer coefficient
k	Thermal conductivity
l	Conduction path length
M	Total number of cells
N	Number of coplanar nearest neighbors

q	Heat flux
q'''	Internal heat generation
s	Distance between patches
T	Temperature
ΔT_{rew}	Calculated critical liquid-solid contact wall superheat at the end of the lifetime of the vapor mushroom bubble
X	Distance
V	Volume

Greek Symbols

ρ	Density
α	Thermal diffusivity
θ	Contact angle
δ	Macrolayer thickness
T	Vapor mushroom hovering period
ΔT	$T - T_{sat}$

Subscripts

av	Surface-time average
CHF	Critical heat flux
d	Dry patch
eff	Effective
h	Heater
hn	Homogeneous nucleation
rew	Rewetting
s	Stem
sat	Saturation

v	Vapor
w	Wall
1	Two-phase macrolayer region
2	Dry-patch region
max,as	Asymptotic maximum value

Acronyms

CHF	Critical heat flux
HTC	Heat-transfer coefficient
STA	Surface-time averaged

I. INTRODUCTION

The development of accurate methods for predicting the critical heat flux (CHF) in boiling processes has been of interest for several decades. The primary reason is that the CHF is the limiting condition of the nucleate boiling region for power-controlled systems. Nucleate boiling is the most efficient region from a heat dissipation standpoint. Yet, despite this long-standing interest in CHF, there is as yet no consensus on the mechanisms that cause CHF, and prediction has remained principally an empirical art.

Various CHF models have been reviewed in many papers, with Unal et al. (1992) presenting one such review. Unal et al. (1992) indicated that studies of CHF can be categorized broadly under four headings: empirical equations, bubble interaction models, hydrodynamic instability models, and surface-controlled models. One drawback of all the modeling efforts is that they are not completely consistent with some experimental observations (e.g., Corty and Foust, 1955; Kirby and Westwater, 1965; Van Ouwerkerk, 1972). These experimenters noted the occurrence of dry areas on

the heater surface while operating in the high heat-flux portion of the nucleate boiling region, well before CHF occurred. Also, at CHF, the macrolayer had not been completely dried out except at the localized dry spots. These observations suggest three things. First, CHF is not the immediate consequence of limited liquid resupply, as suggested by the hydrodynamic instability model, because significant liquid remains on the heater surface. Second, because macrolayer evaporation is not complete over the entire heater surface at CHF, CHF is not the immediate consequence of the dryout of the macrolayer, as postulated by the surface-controlled model. Third, complete macrolayer evaporation can be very localized.

Unal et al. (1991, 1992) proposed that localized dryout of the macrolayer is a necessary condition only for the occurrence of CHF and is not a sufficient condition. They suggested that in addition to the dryout of the macrolayer, some point on the heater surface must reach a temperature high enough to prevent further rewetting of that point. When this occurs, as in the case of power-controlled heaters, the temperature of the hot spot increases continuously, resulting in a runaway condition called the CHF. This hypothesis is really an extension of the surface-controlled model and unifies both the mechanisms of CHF and quenching by relating them to the ability of liquid to rewet the heater surface. It also considers the conduction process within the heater and introduces, in a natural manner, the effects of heater thermal properties, as well as heater thickness on the CHF. In addition, it retains the influence of the hydrodynamics through the liquid resupply mechanism.

To investigate the "hot-spot" hypothesis, Unal et al. (1991, 1992) used the pool boiling data of Gaertner (1965) for water boiling on a horizontal heater and calculated the critical rewetting temperature—the temperature that the hot spot must reach before further rewetting is prevented. This was done by formulating a two-dimensional transient heat conduction model for the heater and its boiling surface. The heater

surface was divided into a circular "dry" region at the center of the heater and a "wet" region surrounding it, as shown in Fig. 1. The dry region is dry only for a portion of the hovering period of the vapor mushroom. Initially, the dry region, as well as the wet region, is covered with the macrolayer, which has numerous vapor stems. But if a localized area on the heater has a thinner macrolayer, this area can dry out at some time during the hovering period. When this localized dryout occurs, the heater surface defined by this area is effectively insulated for the remainder of the hovering period. The "nucleate boiling" heat transfer that occurs in the wet region was represented by a heat-transfer coefficient (HTC), h_2, which was evaluated using the model of Pasamehmetoglu et al. (1993). The heat transfer that occurs over the thinner macrolayer regions between the start of the hovering period and the time at which dryout occurs was represented by an HTC, h_1. Calculation of this HTC was also done using the method of Pasamehmetoglu et al. (1993).

The effect of the choice of the initial macrolayer thickness on h_1 is determined by carrying out the calculations for several plausible values. Calculations show that the critical rewetting temperatures varies between 156.6 and 182.5°C for initial macrolayer thicknesses ranging between 11 and 0 μ, respectively. This provides an indication of the relative importance of the local macrolayer thicknesses on the critical rewetting temperatures, and thus on CHF. The reader is referred to Unal et al. (1991, 1992) for complete details.

In a subsequent study, Unal et al. (1993) investigated the influence of nucleation site density and contact angle on CHF within the hot-spot hypothesis. Using the data of Wang and Dhir (1991), the nucleation site density was found to have a significant effect on the CHF. Also, using the data of Gaertner (1965) for water-nickel-salt solutions, which have low contact angles on copper surfaces, Unal et al. (1993) found that the

calculated rewetting temperatures were again in good agreement with the contact-angle-dependent rewetting temperature data of Ramilison and Lienhard (1987).

Despite these successes, one perceived drawback of the approach used in these studies is the assumption that the heat conduction process was two-dimensional. The dry patch was assumed to be circular and concentric with the heater itself. Intuitively, it might seem that this is a rather stringent idealization. After all, the dry spot is formed as the result of localized dryout of the macrolayer. Localized dryout, in turn, is the consequence of the fact that localized regions of the macrolayer are thinner than other regions. The formation and thickness of the macrolayer is related ultimately to the distribution of active nucleation sites on the heater surface (see Sadasivan et al., 1992). Thus, we believe that the formation of dry patches is related to the active site distribution. Because the active site distribution is in general rather irregular, we can expect that the dry patches formed will be irregular as well. That is, they need not be circular; furthermore, there could well be multiple dry areas on the heater surface. Clearly, if we are to undertake a more realistic examination of the phenomenon, we should be considering the three-dimensional problem. This will obviate the need for making stringent idealizations on the geometry and distribution of the dry areas.

The primary objective of this study is to investigate the hot-spot-controlled CHF hypothesis using a three-dimensional heat conduction model and to elucidate the effect of dry-patch location and shape (which corresponds to the physical distribution of active nucleation sites on the heater surface) and dry-patch distribution (multiple patches) on the rewetting temperature. The results can be used to determine the relative inaccuracies possibly introduced into the calculations in the earlier studies (Unal et al., 1991, 1992, 1993) as a result of assuming a two-dimensional geometry and a single-circular dry patch.

A further objective is to compare the effects of dry-patch shape and multiple dry-patch interactions on the rewetting temperature with the corresponding effects of initial macrolayer thickness. Testing the sensitivity of the calculated values of the rewetting temperatures to these effects will shed further light on the validity of the hot-spot-controlled CHF hypothesis.

II. HEAT-TRANSFER MODEL

The three-dimensional heat conduction problem has been formulated to study the heat-transfer process that occurs in the high-heat-flux, nucleate-boiling region. A computationally efficient supercomputer code named MACRO3D was developed for this purpose. The code uses a three-dimensional control volume discretization scheme to represent the solution domain—the composite structure comprised of the heater and, if desired, a liquid macrolayer. The algebraic equations used to represent the system are obtained by carrying out energy balances on each individual control volume. The scheme is strictly conservative because when a specified quantity of energy enters one control volume from a neighboring one, the latter loses precisely the same quantity of energy. The code employs lumped control volumes; system parameters such as temperature, thermophysical properties, etc., are assumed to be invariant over each control volume, and no element-based interpolation functions need to be specified.

The control volumes have polygonal cross sections (in the radial plane) and have vertical faces in the axial plane. A sample element configuration is shown in Fig. 2 for a circular heater with an circular dry patch. Complete details of the mesh generation method employed are provided by Sadasivan et al. (1993). One feature of the mesh configuration used in the code is that the mesh can include variable-shaped elements; that is, the polygonal elements employed do not all have to have the same number of sides. In a lumped scheme, it is desirable to have a cell communicate directly with as

many neighboring cells as possible. This could be achieved reasonably well by using a uniform mesh made up of, say, hexagons, but in this case, the vapor-liquid boundaries will be discontinuous because they will have to follow the edges of the hexagons. This problem is ameliorated considerably in the present code by using cells with varying numbers of sides. Thus, a given vapor-liquid boundary can be approximated by a reasonable number of straight-line segments, and cells are generated in this area in such a manner that these segments form the sides of the cells. Also, the granularity of the mesh can be varied from one location on the heater to another relatively easily. Thus, any dry-patch shape could be specified on the heater surface. As we will discuss later, elliptical dry patches are considered in this paper. The coordinates of the ellipse boundary and the heater's outer boundary are input to the mesh generation program.

For purposes of evaluating diffusive flows across the face of each control volume, the system parameters are assigned to the center of each control volume, and the internodal distance is used as the characteristic length across which diffusion occurs. This is facilitated by the fact that the common face between two control volumes across which diffusion takes place is normal to the line that connects their centers. The estimation of the energy transfer between the two sets of control volumes across the interface requires the specification of a methodology for prescribing the effective diffusion coefficient across the discontinuity. The effective diffusion coefficient is calculated by using a harmonic mean of the diffusion coefficients of the control volumes across the interface. That is,

$$k_{eff} = \frac{1}{\frac{1-f}{k_i} + \frac{f}{k_{i+1}}}, \tag{1}$$

where f is the ratio $l_i/(l_i + l_{i+1})$. This scheme was based on the steady one-dimensional, no-source heat conduction situation in which the conductivity varies in a stepwise manner from one control volume to another. However, the scheme has also been

shown to provide better results for more complicated cases, as well (see Patankar, 1980). For this reason, the harmonic mean approach has been used in this work.

A. Governing Equations

The basis of the solution is the differential form of the conservation of energy,

$$\text{Div}\,(k\ \text{grad}\ T) + q''' = \frac{\partial}{\partial t}(\rho\ C_p\ T)\ . \tag{2}$$

By integrating Eq. (1) over a control volume V, we get

$$\int_V [\text{Div}\,(k\ \text{grad}\ T) + q'''] \, dV = \int_V \frac{\partial}{\partial t}(\rho C_p\ T)\, dV\ . \tag{3}$$

Further, applying the divergence theorem

$$\int_A k(\text{grad}\ T)\, dA + \int_V q'''dV = \int_V \frac{\partial}{\partial t}(\rho\ C_p\ T)\, dV\ , \tag{4}$$

one can obtain a conservative lumped parameter approximation to Eq. (2) for the temperature at any node

$$A_i\, k_i \frac{\Delta T_i}{\Delta x_i} + V_j\, q_j''' = V_j\, \rho_j\, C_{pj} \frac{\partial T_j}{\partial t}\ \ , j=1,M\ , \tag{5}$$

where the subscript j refers to the node under consideration, and subscript i refers to the lumped quantities in each of the neighboring nodes of node j. Thus, for a polygon cell, as shown in Fig. 2, each cell has N number of coplanar nearest neighbors, and Eq. (5) becomes

$$\sum_{i=1}^{N+2} A_i\, k_i \frac{T_i - T_j}{\Delta x_i} + q'''V_j = V_j\, \rho_j\, C_{pj} \frac{T_j^{n+1} - T_j^n}{\Delta t}\ , j=1,M\ , \tag{6}$$

where $q'''Vj$ is a source term that accounts for the internal generation (assumed to be zero in the present case) and the boundary conditions.

From Eq. (6),

$$T_j^{n+1} = T_j^n + \Delta t \left[\sum_{i=1}^{N+2} \frac{\alpha_i A_i}{V_j \overline{\Delta x_i}} (T_i - T_j) + q'''_j \right], \tag{7}$$

where $\overline{\Delta x_i}$ is the distance between the center of node j and each of its neighbors, and α_i is the thermal diffusivity. In the present analysis, the properties are assumed constant.

B. Boundary Conditions

Consistent with thick heater experiments, a constant heat-flux boundary condition can be imposed on the lowest level of cells, as shown in Fig. 2, and the top surface cells are subjected to a convective boundary condition. Further details on this aspect are provided in the next paragraph. The heat flux owing to these boundary conditions is accounted for by representing these conditions as additional volumetric heat source components in the boundary cells. The heat-transfer coefficient (HTC), the imposed heat flux, and other parameters can be specified for each individual cell at each timestep, thus permitting a full three-dimensional transient treatment of the heat conduction process. The source term, q'''_j, describes the boundary conditions and/or internal heat generation that was assumed to be zero in this paper. The convective heat transport at the top of the heater (see Fig. 3) is computed as a volume-averaged heat-generation term by

$$q'''_j = \frac{h_i A_{ij} (T_{sat} - T_j)}{V_j} . \tag{8}$$

See Sadasivan et al. (1993) for more details. At the bottom of the heater, the constant heat-flux boundary condition is expressed as

$$q'''_j = \frac{q_j A_j}{V_j} \quad . \tag{9}$$

C. Numerical Scheme and Accuracy

For a semi-implicit solution of the system of Eq. (6) written for all the elements, the right-hand side of Eq. (6) is expressed as the average of the terms evaluated at the current timestep and those evaluated at the previous timestep. For a general problem being solved using MACRO3D, an implicit or semi-implicit scheme such as the one used here requires the solution of a large sparse linear system of algebraic equations. The coefficient matrix of this system is not symmetric and positive definite (SPD); therefore, commonly used methods for SPD systems such as the conjugate gradients (CG) algorithm are not applicable. A number of modifications of the CG algorithm have been proposed to enable the solution of non-SPD systems. For the present study, the conjugate gradient squared (CGS) method was chosen as the solution algorithm (see Rider et al., 1991).

The use of a lumped-parameter approach results in a conservative estimate of surface temperatures. Ball (1976) points out that these errors become higher as the value of the parameter $2\alpha\Delta t/\Delta x^2$ tends to zero. Thus, we can expect that a more accurate solution can be obtained by using small values of Δx and/or larger values of Δt. A series of test calculations was carried out to verify the effect of temporal and spatial nodalization on the accuracy of the solution.

Test problems used a regular hexagonal mesh scheme. A representative problem was solved using a 188-cell grid, as well as a 333-cell grid. Both calculations were terminated after 150 hovering periods, using a timestep size of 1 ms. The results at the end of 150 periods were compared and were found to differ only insignificantly. This implies that a 188-cell grid, which is a typical number for calculations considered in this

paper, could be used without a significant loss of accuracy. Similar tests were performed to determine the effects of axial node size and timestep. With an axial node size of 0.1 mm and timestep of 0.1 ms, the solution did not change significantly with a further decrease in the axial node size and timestep. All calculations were done on a CRAY Y-MP vector supercomputer. The truncation error and its propagation is very negligible for this Cray machine, which uses a 64-bit word representation. The 14th digit of a real number is ensured to be correct. By performing a calculation with double precision, the accuracy of representing a real number can be increased. However, this would result only in a change in the fourth or fifth digit after the decimal point for the temperature ranges of interest in this paper. Therefore, the truncation error and its propagation are negligible for the present calculations.

D. Heat-Transfer Model for Second Transition Region of Nucleate Boiling

For the present problem, the sketch of the heater and the boiling surface is depicted in Fig. 2. The boiling surface is the top surface of the heater and consists of dry and wet regions. In this paper, as in Unal et al. (1993), we assume that the dry patch forms in an infinitesimally short period of time with only enough liquid present to rewet/quench the heater surface. Therefore, the boiling surface always includes a dry region. Physically, the wet region consists of numerous vapor stems with liquid macrolayers. The transient HTC on the wetted region of the heater surface is obtained using the method of Pasamehmetoglu et al. (1993) based on the experimental data of Gaertner (1965) for the pool boiling of water on a copper heater. At each timestep during a hovering period, the HTC for that time is applied to each of the heater surface cells that are on the prescribed wet region. The variation of the wet-side heat-transfer coefficient over one hovering period is shown in Fig. 3. The surface cells located on the designated dry areas are assumed to be adiabatic. Starting with an arbitrary initial temperature distribution, calculations are carried out for successive hovering periods.

The calculations are terminated when the solution becomes stationary—that is, when the surface- and time-averaged (STA) temperatures and heat fluxes over a hovering period are within a specified tolerance level of those evaluated over the previous hovering period.

III. RESULTS AND DISCUSSION

The initial phase of this study validated the new computer program using numerous test problems (Sadasivan et al., 1993) and by repeating the earlier two-dimensional concentric dry-patch calculations made by Unal et al. (1991, 1992). This configuration is illustrated in Fig. 2. The heater and dry-patch diameters were specified as 0.051 m and 0.0364 m, respectively, to represent Gaertner's (1965) experiment. The new calculations found that a surface dry-area fraction of 0.51 resulted in the same STA temperature as the experimental value. The rewetting temperature was found to be 183.0°C, which is very close to the original value of 182.6°C obtained in the two-dimensional calculations. In addition to validating the three-dimensional solution and establishing a common reference point for comparison, the calculation shows that the granularity of the irregular mesh causes no loss of accuracy.

A. Effect of Single-Patch Location and Shape

We considered a two-dimensional concentric single dry patch that is circular in shape in the previous paragraph. The first thing we will examine is the sensitivity of the rewetting temperature to the location of the circular dry patch. To examine this effect, a circular eccentric dry patch will be considered, as shown in Fig. 4. The configuration shown in Fig. 4 represents almost the worst possible eccentricity; the center of the dry patch is located 6.3 mm from the center of the circular heater. This configuration permits a very small wet region (about 1 mm in width) at the right side of the dry patch. The ratio of the dry to wet areas is exactly the same as the value we used

in our two-dimensional concentric circular dry-patch model. For this eccentric configuration, the calculated rewetting and the STA temperatures increased from 183.0 and 43.4°C to 189.1 and 45.84°C, respectively, indicating an insignificant change. These results indicate that as long as a wet region surrounds the dry patch, the heater surface temperature distribution is not sensitive to the precise location of the dry patch.

Having shown that the location of the patch on the heater is not significant, we locate the patches at the center of the heater to simplify the calculations through the use of quarter symmetry and then relax the circular shape requirement. We will use the ratio of the major axis to the minor axis of the ellipse (aspect ratio) to characterize the shape of the ellipse, as shown in Fig. 5. For the cases reported here, we varied the aspect ratio from 1.0 (circular) to about 10.0. Two grid structures were used in these calculations. An irregular grid structure is shown in Fig. 2, and a hexagonal grid structure is shown in Fig. 6. The irregular grid structure provided the capability to represent the interface between the dry patch and the wet regions on the heater in a very precise manner, thus accurately representing the elliptical shape and area. The hexagonal grid, while not representing this wet-dry interface as accurately, provided longer computational vector lengths and thus ran faster on the computer.

The calculational procedure adopted selected the size of the dry area and then performed calculations for various values of the aspect ratio. We will use two different terms for the highest temperature in the dry area: the rewetting temperature and the hot-spot temperature. Rewetting temperature is used to refer to the highest temperature on the heater surface obtained in calculations concerning the actual experimental situation. An example of this is the case where the void fraction is equal to 51% and the STA temperature is equal to Gaertner's (1965) experimentally measured value 0f 43.4°C. Hot-spot temperature, on the other hand, is used to refer to the highest temperature on the heater surface that is obtained in any general calculation, the

condition of which does not necessarily correspond to actual experimental situations. Such calculations have been carried out to identify the influence of shape, void fraction, etc., better. We remind the reader at this point that the rewetting temperature at the onset of CHF is actually a unique value for a given heater-fluid combination. When we talk about the effect of a parameter, such as the initial thickness, the dry patch size or the number of dry patches, on the rewetting temperature, we do not imply that "the rewetting temperature is multivalued." We mean to indicate the effects of assumptions we made in our model. In other words, the variation in calculated values of rewetting temperature can be used as a measure of "goodness" of the model for a given heater-fluid. For example, in our previous papers, we calculated the rewetting temperature using a 2-D model for a given initial macrolayer thickness in the dry area. It was shown that a range of rewetting temperature can be obtained for a range of initial macrolayer thickness. As we explained in the introduction, the shape and number of dry patches considered in the model could affect the calculated rewetting temperature. In this paper, we explicitly investigated how sensitive the rewetting temperature is to the shape and number of patches. Furthermore, we want to verify that the resulting possible range for the rewetting temperature still supports the hot spot controlled hypothesis; i.e., the mechanism of occurrence of CHF is controlled by the rewetting of hot surfaces. Thus, for each fixed dry-area size (and consequently, the area void fraction $A_d/A_{w)}$, the STA and hot-spot temperatures for the converged hovering period vary as the dry-patch shape is changed. Results of these calculations are included as Table I and are shown in Fig. 7. Results of both grid structures are presented together, and little sensitivity was found to the exact representation of the wet-dry interface.

Figure 7 shows that the hot-spot temperature is less sensitive to the shape of the dry patch for lower void fractions (A_d/A_w). Changing the aspect ratio up to 10 varies the hot-spot temperature about 6°C for void fractions of 0.04 to 0.11. For high void

fractions, the aspect ratio is limited to about 2.5 owing to the limited heater surface area. The hot spot temperature decreases as much as 10°C as the aspect ratio increases. At the CHF conditions at which the void fraction was determined as 51%, the rewetting temperature shows only 2°C change when the dry-patch shape is changed from a circle to an ellipse with an aspect ratio of 1.47. This reveals that for the conditions of Gaertner's (1965) experiment, the calculation of the rewetting temperature would not be affected by the shape of the dry patch as long as there is only a single patch on the heater surface.

The aspect ratio could not be changed by small increments for high void fractions owing to the grid sizes. However, one can correlate the hot-spot and STA temperatures in Table I as a function of the semiminor (a) and semimajor (b) axes of the ellipse, using the high void fraction data (higher than 30%). Then, at CHF (specified by a STA temperature of 43.4°C), the rewetting temperature can be evaluated for various values of a and b. Note that the dry-patch area is πab. This is nothing but the interpolation of calculated data. Figure 8 shows the results obtained from such a correlation. It shows that the rewetting temperature difference between ellipse-circle and strip-circle configurations give the same STA temperature as a function of the semiminor axis of the ellipse. The semimajor axis of the ellipse is also plotted in the figure. There is only one point for the strip dry-patch geometry, and the aspect ratio becomes infinitely large for this case. Figure 8 clearly demonstrates that the rewetting temperature is not sensitive to the shape of the dry patch for an ellipse-circle configuration; the change is only 1.5°C. For a strip-circle configuration, the difference becomes 8°C, also showing an insignificant effect. From the above results, we can conclude that the sensitivity of the rewetting temperature to the shape of the dry patch can be neglected in the case where only a single patch can exist in the heater surface. Gaertner (1965) did not mention whether there was a single patch or multiple patches on the surface. We will investigate

the multiple-patch case and its effect on the rewetting temperature in the following section.

Because the results presented using the regular hexagon grid scheme do not cause any loss in accuracy, whereas using the grid scheme cuts the computational time significantly, we will use a uniform hexagonal grid scheme for the calculations concerning the multiple-patch interaction.

B. Effect of Multiple Dry Patches

An assumption made in the previous studies is that only one dry patch forms on the heater surface. If there are multiple patches on the surface, their interaction may affect the heat conduction process within the heater, thus altering the heater surface temperatures. The effect of multiple patches will be assessed in this section.

In the first set of calculations, the dry-patch shapes are chosen in such a manner that their aspect ratios are greater than 3.0. This is in accordance with the results of the previous section that show that beyond this limiting value, there is no effect of shape on the rewetting temperature. This will help to isolate the effect of multiple patches on the rewetting temperature in these calculations. Two identical patches with the same aspect ratio are located on the heater, and the separation distance between them is varied in successive calculations. The sequence is then repeated for another aspect ratio. Selected results are listed in Table II. A typical dry-patch configuration used in the calculations is shown in Fig. 9.

For each set of runs keeping the area of the dry patches the same, the rewetting temperature tends to reach an asymptotic value as the spacing between the patches is increased. Figure 10 is a plot of the ratio of the rewetting temperature to the corresponding high-spacing asymptotic value, plotted as a function of the spacing

between the patches. Figure 10 indicates that the effect of multiple-patch interaction is minimal at worst—for cases where the spacing between the patches is relatively small compared to the dimensions of the dry patch, the calculated rewetting temperatures are up to 4% higher than the asymptotic values. The magnitude of the effect is of the same order as the effect of dry-patch shape discussed in the previous section. As the spacing increases, this effect is further reduced. Again, these calculations have shown that the effect of dry-patch interaction is minimal, especially for dry patches with large aspect ratios.

The question of multiple dry-patch interaction can be posed another way. Given a measured STA heater surface temperature [in this case, Gaertner's (1965) experimental value of 43.5°C], can we have more than two dry patches on the heater surface without changing the rewetting temperature appreciably? If so, is there an upper limit to the number of such patches? To investigate this, we increased the number of patches incrementally with the same shape (circular) and size, distributed symmetrically on the heater surface. Also, we adjusted the size of the patches to match Gaertner's (1965) STA measured wall temperature. The results of this calculation are summarized in Table III. We can see that to obtain an STA temperature of 43.4°C (within a ±0.4°C tolerance level), the maximum possible number of patches is four. This configuration is shown in Fig. 11. If we have more than four dry patches on the surface, the STA temperature will not reach this value.

In the case of the four dry patches, the critical rewetting temperature at the center of each patch is calculated to be 162°C, as opposed to 183.3°C obtained for the case of a single patch. This hypothetical case indicates that the number of patches on the surface is important in determining the rewetting temperature. Comparison of the numerical results with those from the previous work (Unal et al., 1991) on the effect of initial macrolayer thickness shows that the two aspects—initial macrolayer thickness and the

number of patches—have approximately the same order of influence on the rewetting temperature. Because the number of patches is ultimately related to the spatial distribution of the initial macrolayer thickness over the heater surface, this further underscores the fact that an accurate treatment of the dry-patch behavior and its role in mechanisms of CHF must include appropriate consideration of the spatial variation in the macrolayer thickness over the heater surface.

The relative importance of the initial macrolayer thickness as compared with the actual shape of the dry patch raises a point regarding the importance of the spatial distribution of active cavities on the heater surface and the size distribution of active cavities on the heater surface. The exact mechanism that determines the initial thickness of the macrolayer is uncertain at this time. However, Sadasivan et al. (1992) suggested that the macrolayer would be thinner in those areas of the heater surface that have many small cavities that are closely spaced as opposed to larger cavities that have a greater spacing. Thus, if the surface preparation method has caused a localized area of closely spaced small cavities (nonhomogeneous cavity distribution), we can expect a dry patch to first develop over this area. Because dry-patch shapes and dry-patch interactions have been shown to have only a second order effect on the surface temperatures, it will matter little whether the resulting dry area is circular, of a more eccentric shape, or whether there are a couple of smaller areas. What this implies is that the methodology we used in determining the possible rewetting temperature at the onset of CHF is not very sensitive to 2-D or 3-D formulation, but rather it is sensitive to the initial macrolayer thickness in the dry areas. However, if the surface preparation method creates a homogeneous cavity distribution over the surface, multiple dry areas might result and these will influence the surface temperatures significantly. In this case, a 3-D formulation of the dry patches as well as the initial thickness become important in

determining the rewetting temperature that is used to verify our hot spot controlled hypothesis for CHF mechanism.

IV. SUMMARY AND CONCLUSIONS

The main conclusions of this study are as follows:

- A three-dimensional heat conduction model has been developed to investigate the behavior of dry patches that develop on the heater surface in high heat-flux nucleate boiling.

- We have examined the effect of the dry-patch shape and the dry-patch location on the calculated values of the rewetting temperatures. The results indicate that these effects are small.

- The effect of multiple-patch interactions has also been investigated. This was done by assuming that two dry areas exist on the heater surface, and the spacing between them was varied in successive calculations. The results indicate that interaction between patches has only a small effect on the calculated values of the rewetting temperatures.

- Another multiple dry-patch case investigated the possibility of having more than two dry patches on the heater surface without changing STA wall temperature. In this case, the rewetting temperature at the center of each patch was calculated as 162°C, as opposed to 183.3°C obtained for the case of a single patch. This hypothetical case indicated that the number of patches on the surface was important in determining the rewetting temperature.

- Comparison of the numerical results with those from the previous work (Unal et al., 1991) on the effect of initial macrolayer thickness indicated that

the two considerations—initial macrolayer thickness and the number of patches—have approximately the same order of influence on the rewetting temperature. Because the number of patches is ultimately related to the spatial distribution of the initial macrolayer thickness over the heater surface, this further underscores the fact that an accurate treatment of the dry-patch behavior and its role in the CHF mechanism must include appropriate consideration of the spatial variation in the macrolayer thickness over the heater surface. Therefore, although a two-dimensional axial-symmetric model would be sufficient from the point of view of dry-patch shape and its spatial distribution, a three-dimensional model is needed for proper consideration of the spatial variation in the macrolayer thickness and the number of patches.

REFERENCES

Ball, S. J., 1976, "ORECA-I: A Digital Computer Code for Simulating the Dynamics of HTGR Cores for Emergency Cooling Analysis," Oak Ridge National Laboratory report ORNL/TM-5159.

Chang, Y. P. and Snyder, N. W., 1960, "Heat Transfer in Saturated Boiling," *Chem. Engr. Prog. Symp. Ser.* **56** (30), pp. 25–38.

Corty, C. and Foust, A. S., 1955, "Surface Variables in Nucleate Boiling," *Chem. Engr. Prog. Symp. Ser.* **51** (17), pp. 1–12.

Gaertner, R. F., 1965, "Photographic Study of Nucleate Pool Boiling on a Horizontal Surface," *Journal of Heat Transfer* **15**, pp. 17–29.

Kirby, D. B., and Westwater, J. W., 1965, "Bubble and Vapor Behavior on a Heated Horizontal Plate during Pool Boiling near Burnout," *Chem. Engr. Prog. Symp. Ser.* **61** (57).

Pasamehmetoglu, K., Chappidi, P. R., Unal, C., and Nelson, R. A., 1993, "Saturated Pool Nucleate Boiling Mechanism at High Heat Fluxes," *International Journal of Heat Mass Transfer*, in press.

Patankar, S. V., 1980, "Numerical Heat Transfer and Fluid Flow," Hemisphere Publishing Company, New York.

Ramilison, J. M. and Lienhard, J. H., 1987, "Transition Boiling Heat Transfer and Film Transition Regime," *Journal of Heat Transfer* **109**, pp. 746–752.

Rider, W. J., Cappiello, M. W., and Liles, D. R., 1991, "Helium Cooled Reactor Analysis Code, Models, Correlations, Validation, and Input Description, " Los Alamos National Laboratory report LA-UR-91-1017.

Sadasivan, P., Chappidi, P. R., Unal, C., and Nelson, R. A., 1992, "Possible Mechanisms of Macrolayer Formation," Pool and Flow Boiling Conference, Engineering Foundation, March 22–27, Santa Barbara, California, *International Communications in Heat Mass Transfer.*, Vol. 19, No. 6, pp. 801–815, November–December, 1992.

Sadasivan, P., Unal, C., and Nelson, R. A., 1993, "MACRO3D, A Three-Dimensional Finite Volume Computer Code for the Analysis of High Heat Flux Nucleate Boiling," Los Alamos National Laboratory report in press.

Unal, C., Vincent, D., and Nelson, R. A., 1991, "Unifying the Controlling Mechanisms for the Critical Heat Flux and Quenching: The Ability of Liquid to Contact the Hot Surface," HTD-Vol. 159, pp. 130–140, 28th National Heat Transfer Conference, Minneapolis, Minnesota (1991).

Unal, C., Vincent, D., and Nelson, R. A., 1992, "Unifying the Controlling Mechanisms for the Critical Heat Flux and Quenching: The Ability of Liquid to Contact the Hot Surface," *Journal of Heat Transfer* **114** (4), pp. 972–982.

Unal, C., Sadasivan, P., and Nelson, R. A., 1993, "On the Hot-Spot-Controlled Critical Heat Flux Mechanism in Pool Boiling of Saturated Fluids," Pool and Flow Boiling Conference, Engineering Foundation, March 22–27, Santa Barbara, California, *Journal of Heat Transfer*, in press.

Van Ouwerkerk, H. J., 1972, "Burnout in Pool Boiling the Stability of Boiling Mechanism," *Int. J. Mass Heat Transfer* **15**, pp. 25–34.

Wang, C. H., and Dhir, V. K., 1991, "Effect of Surface Wettability on Active Nucleation Site Density during Pool Boiling of Water on a Vertical Surface," HTD-Vol. 159, pp. 89–96, 28th National Heat Transfer Conference, Minneapolis, Minnesota (1991).

List of Figures

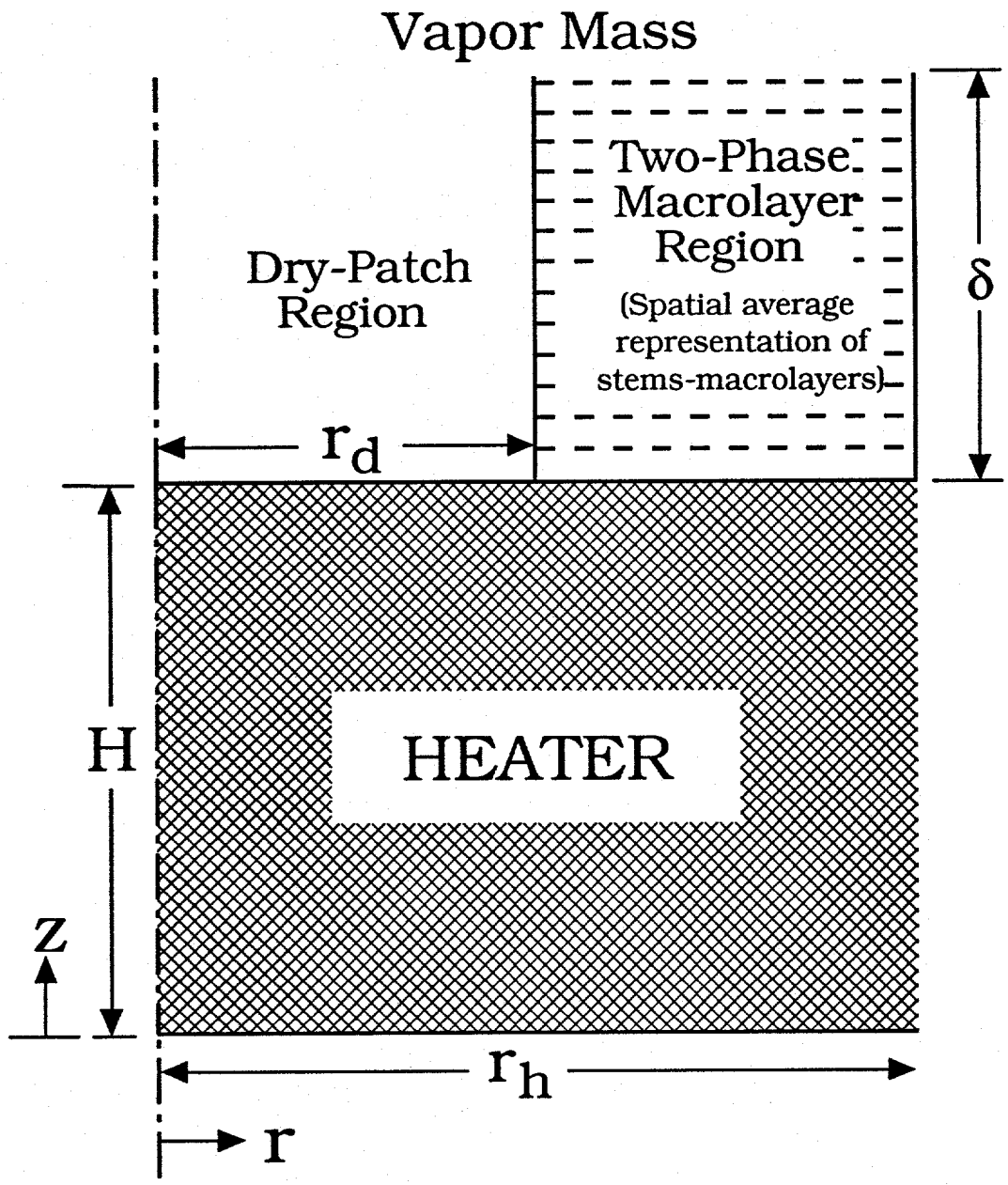

Fig. 1. Two-dimensional heat-transfer model used in Unal et al., 1991.

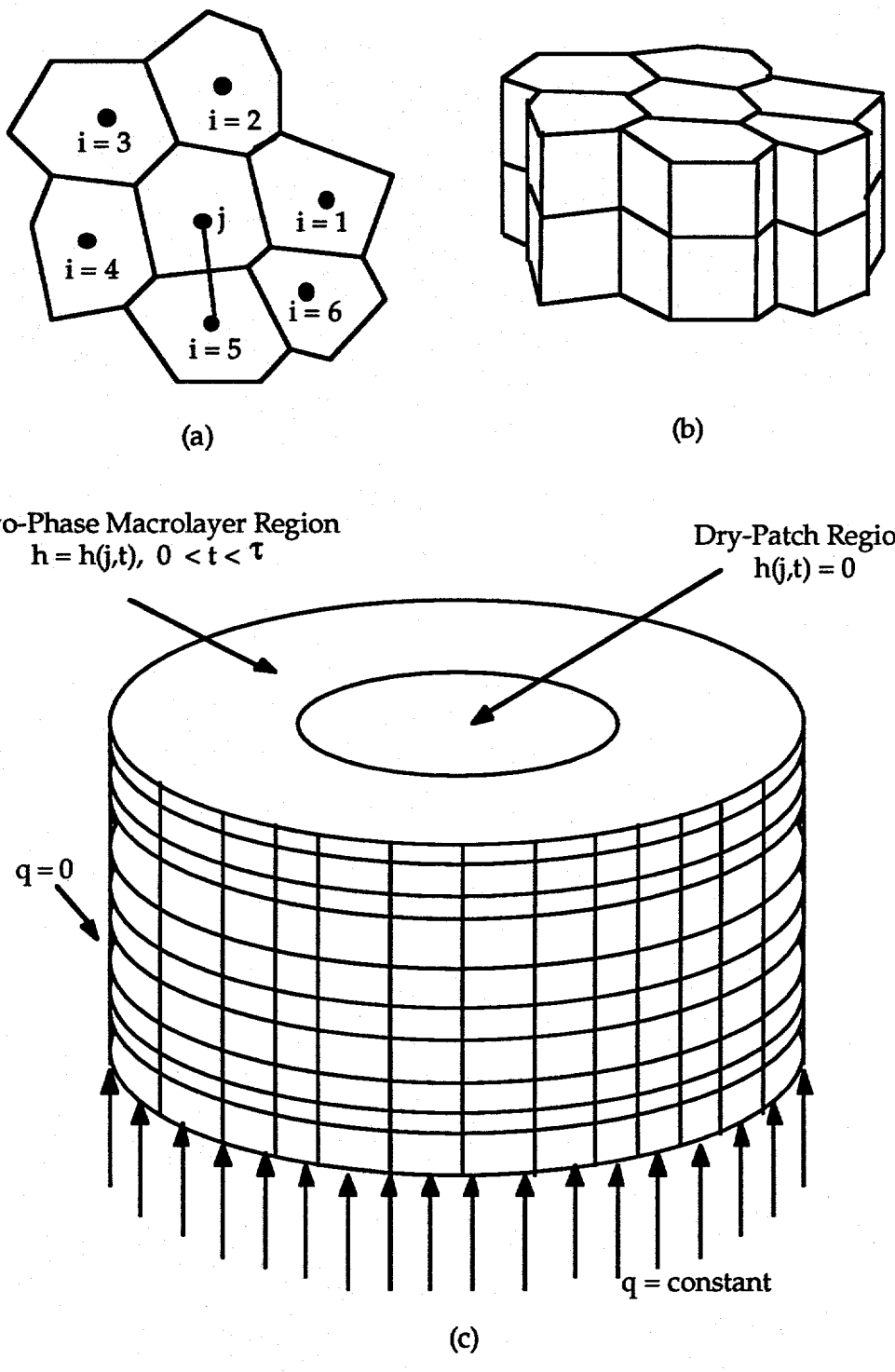

Fig. 2. Sketch of the three-dimensional heat-transfer model and grid structure for irregular mesh: (a) top view of grid, (b) side view of grid, and (c) heater geometry.

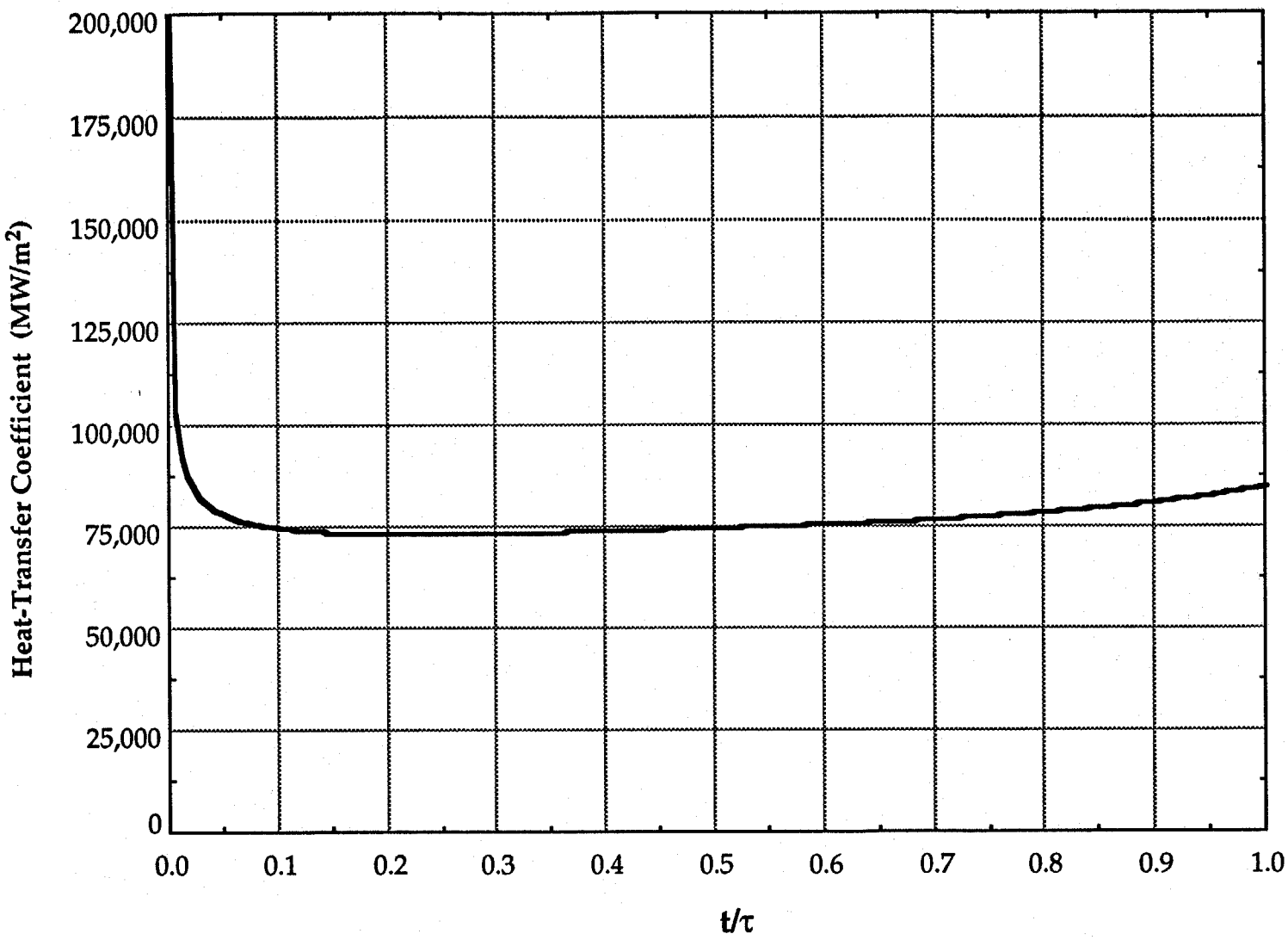

Fig. 3. Variation of surface-averaged heat-transfer coefficient during one hovering period.

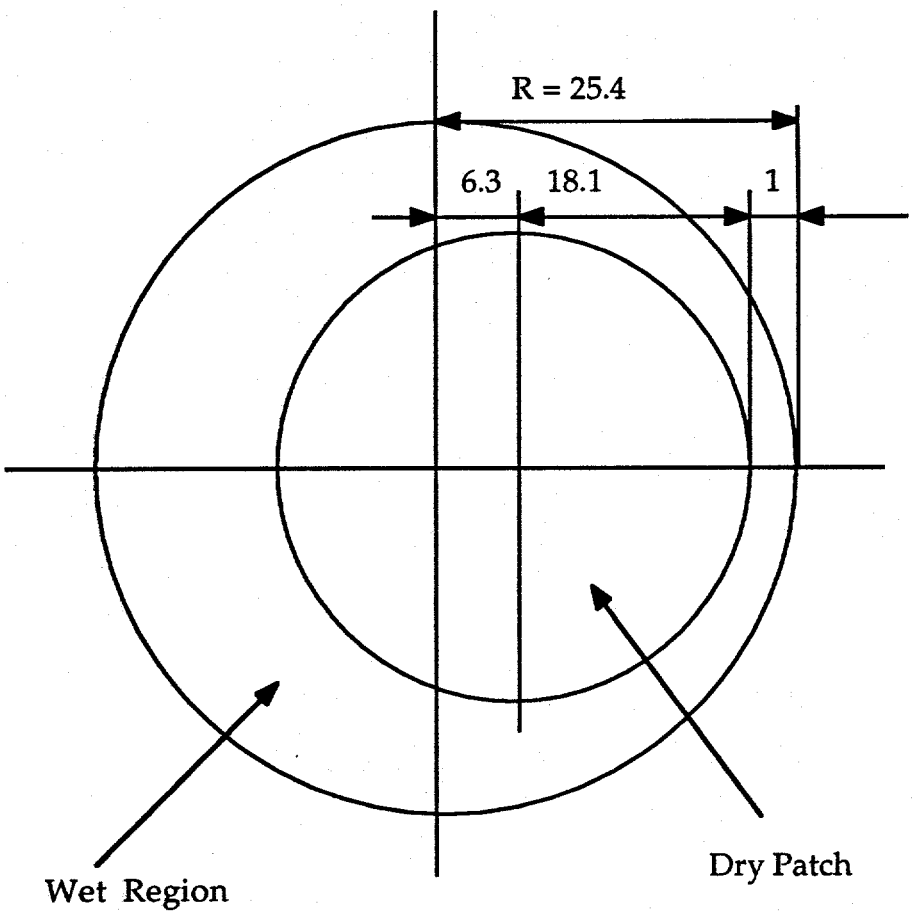

(all dimensions are in mm)

Fig. 4. Sketch of the eccentric dry patch.

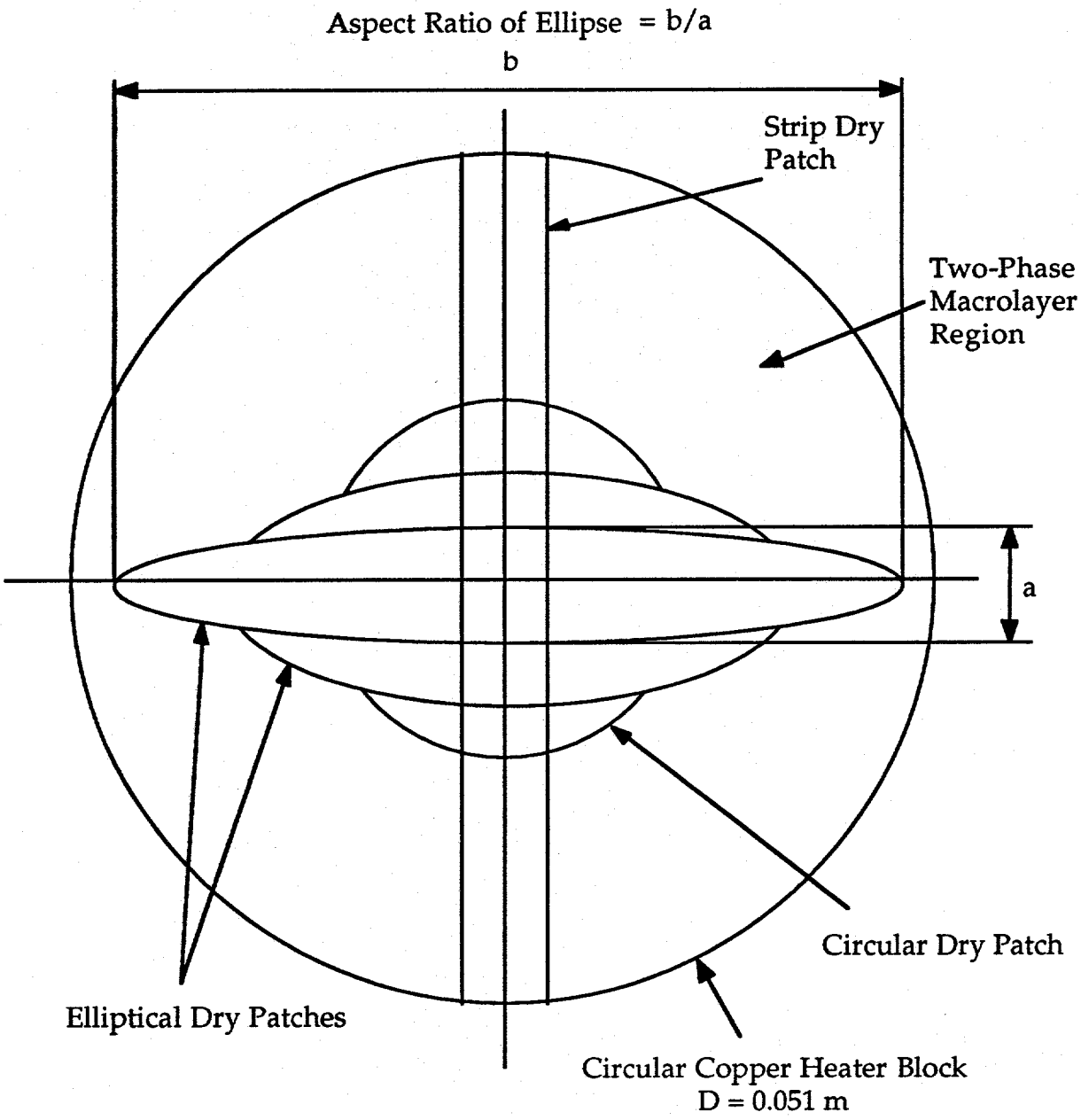

Fig. 5. Schematic of circular and elliptical dry patches.

$$\frac{b}{a}=2.23 \qquad N_{\text{Dry Cells}}=82 \qquad \frac{A_{\text{Dry}}}{A_{\text{Total}}}=0.488$$

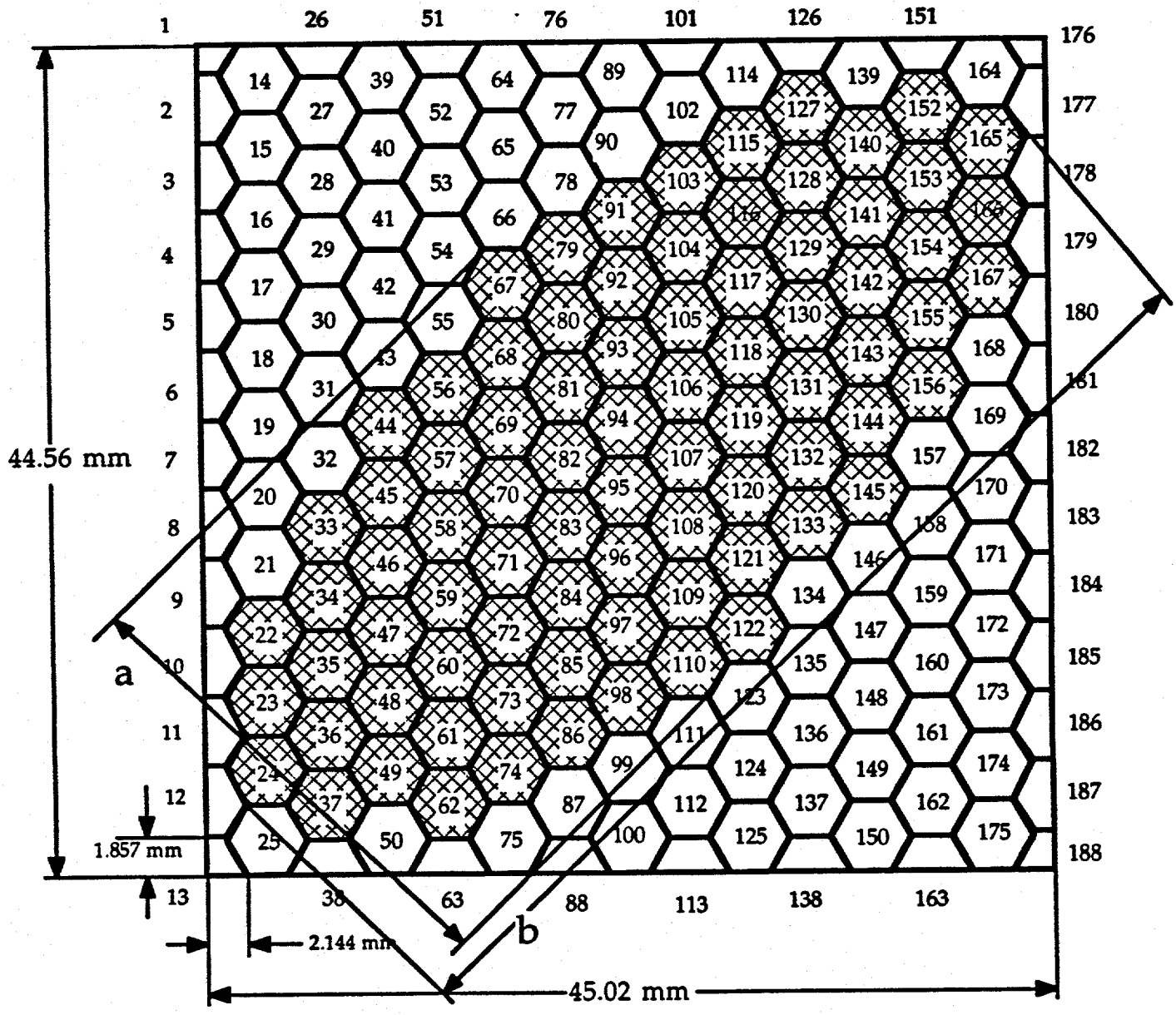

Fig. 6. Boiling surface with an elliptical dry patch using a regular hexagonal grid scheme.

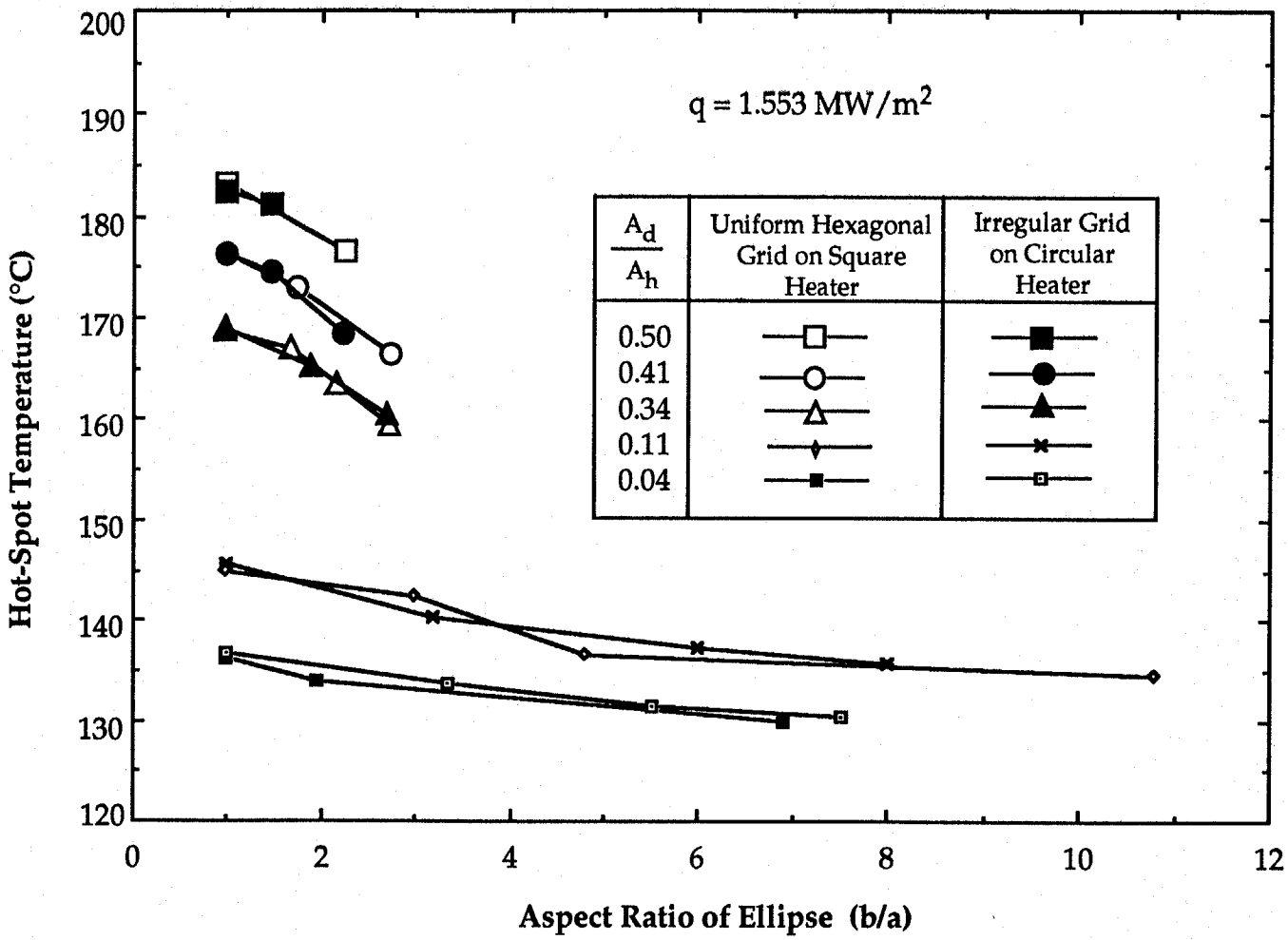

Fig. 7. Hot-spot temperatures as a function of aspect ratio of ellipse for different void ratios using uniform hexagonal and irregular grid schemes.

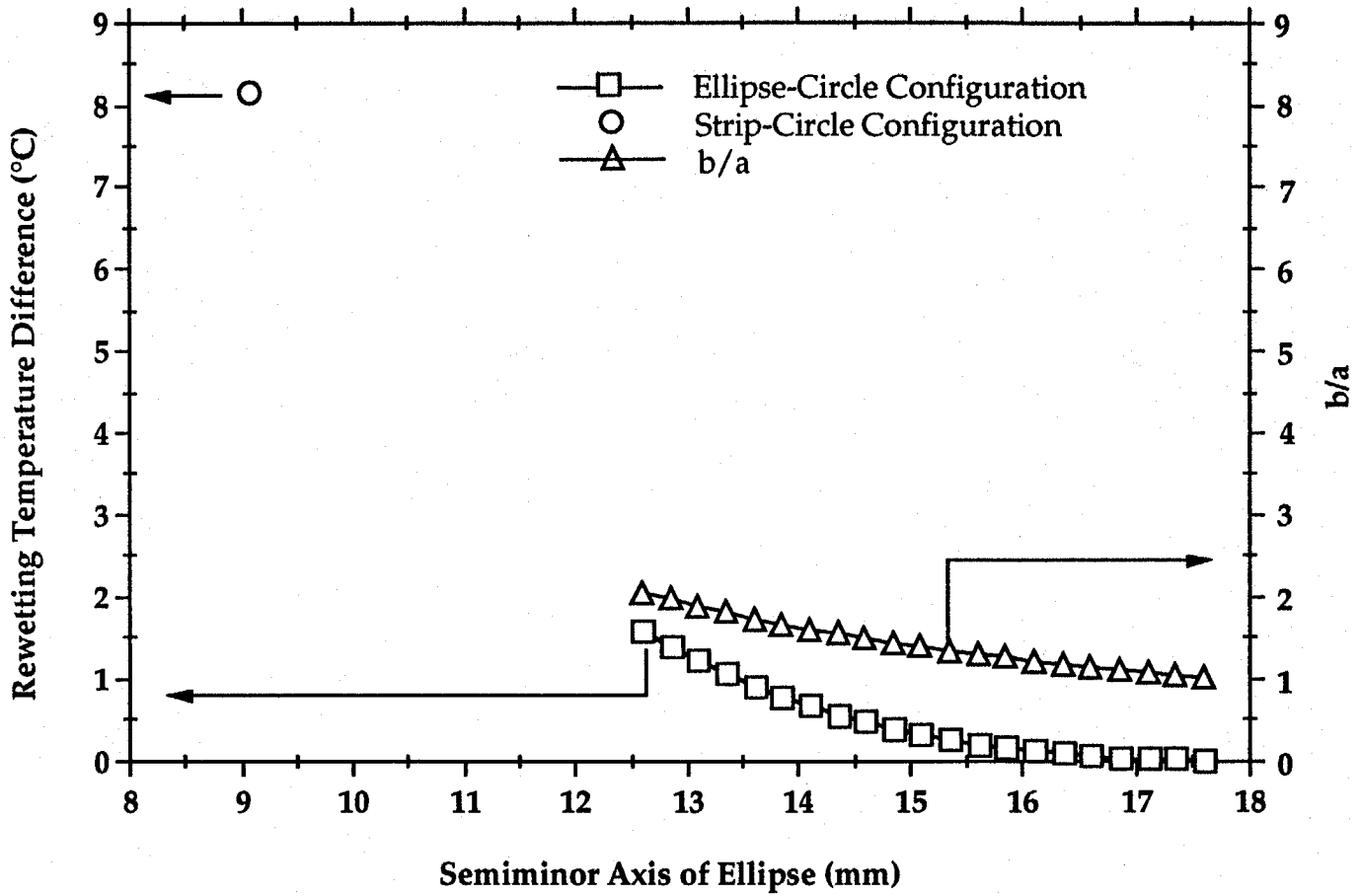

Fig. 8. Variation of maximum patch temperatures as a function of aspect ratio of an ellipse for various dry-patch area ratios using irregular and regular grids.

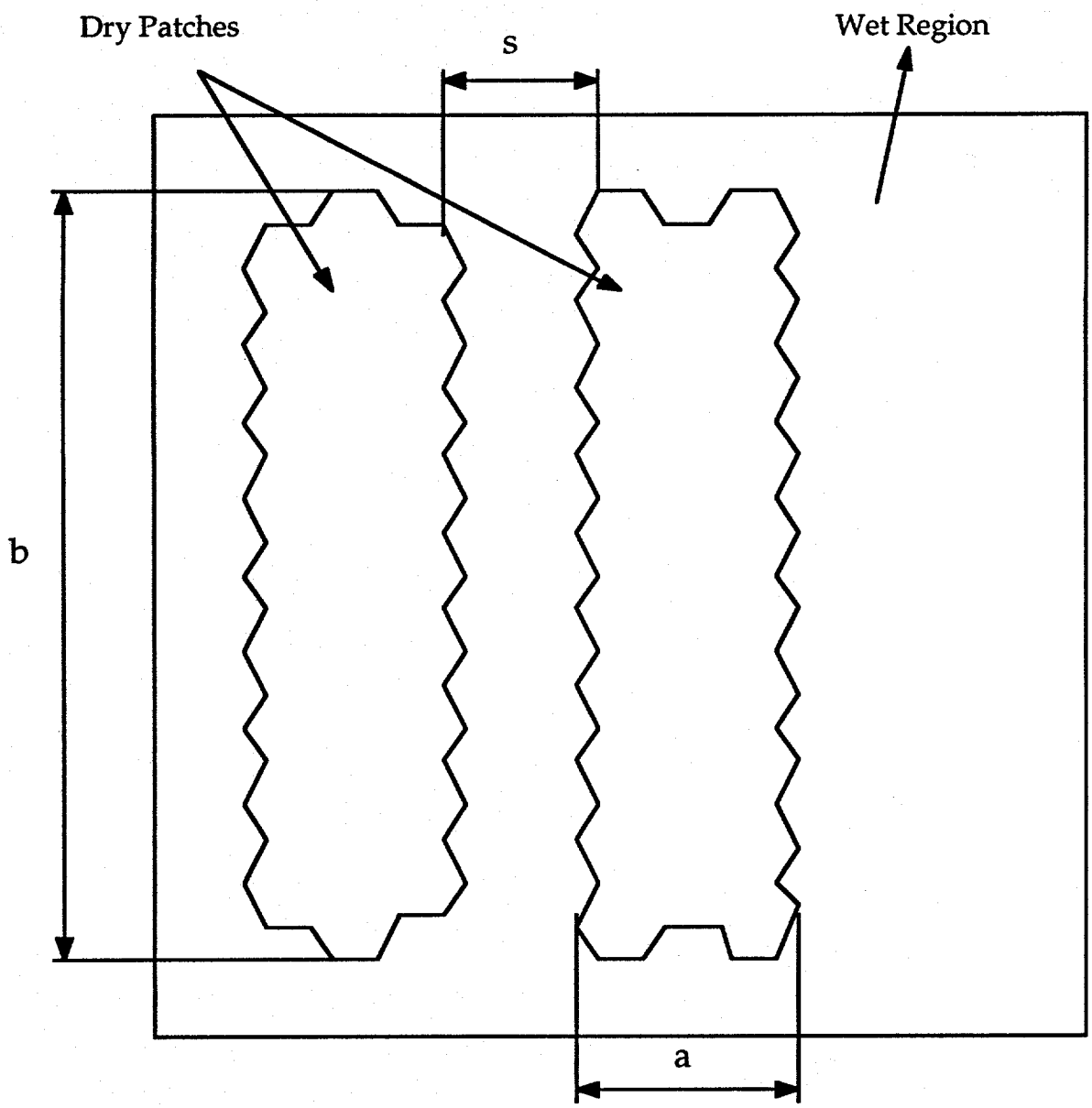

Fig. 9. Sketch of two dry patches on a square boiling surface using the regular hexagonal grid scheme.

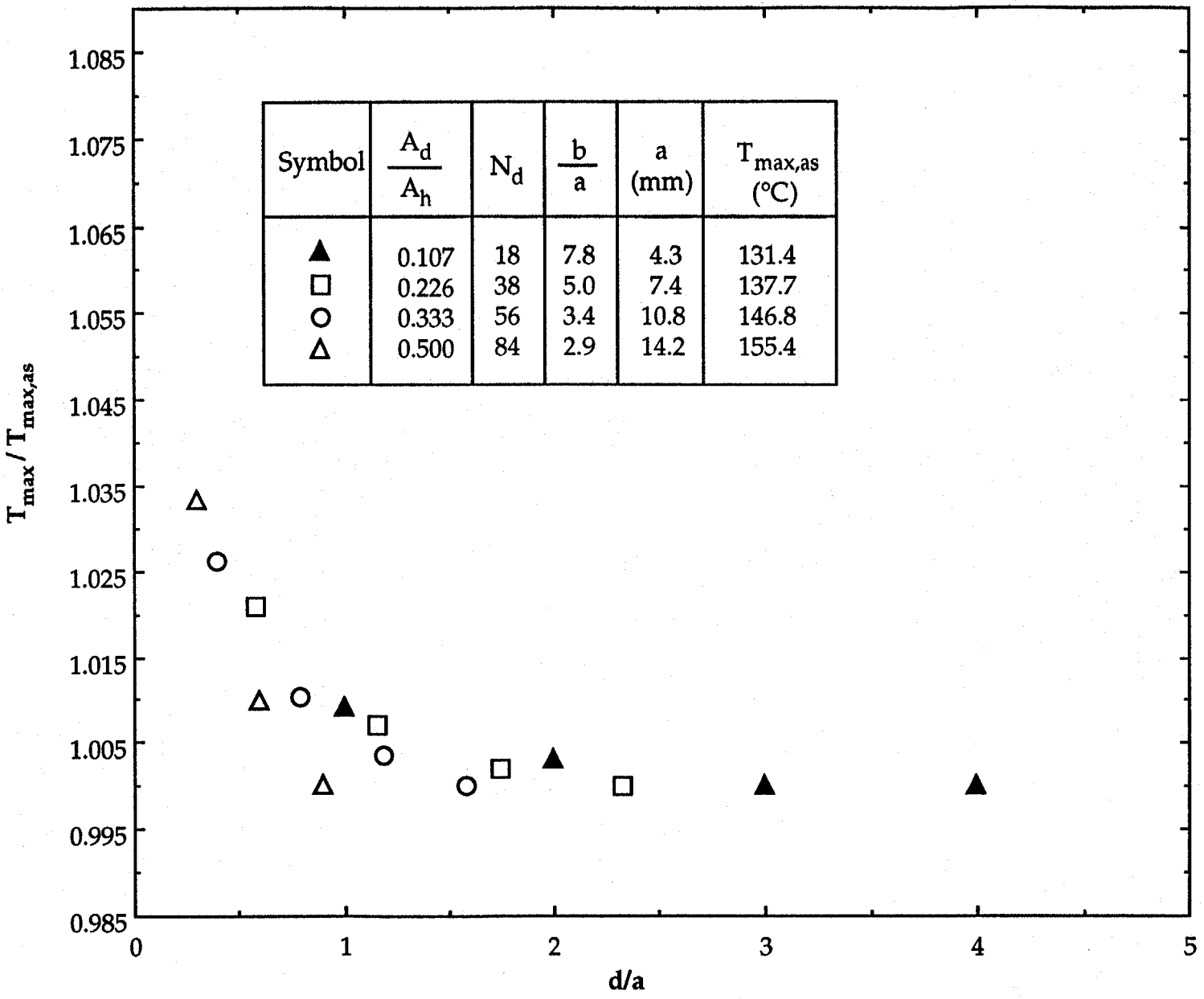

Symbol	$\frac{A_d}{A_h}$	N_d	$\frac{b}{a}$	a (mm)	$T_{max,as}$ (°C)
▲	0.107	18	7.8	4.3	131.4
□	0.226	38	5.0	7.4	137.7
○	0.333	56	3.4	10.8	146.8
△	0.500	84	2.9	14.2	155.4

Fig. 10. Variation of maximum patch temperatures as a function of distance between patches for various dry-patch area ratios using the regular hexagonal grid scheme.

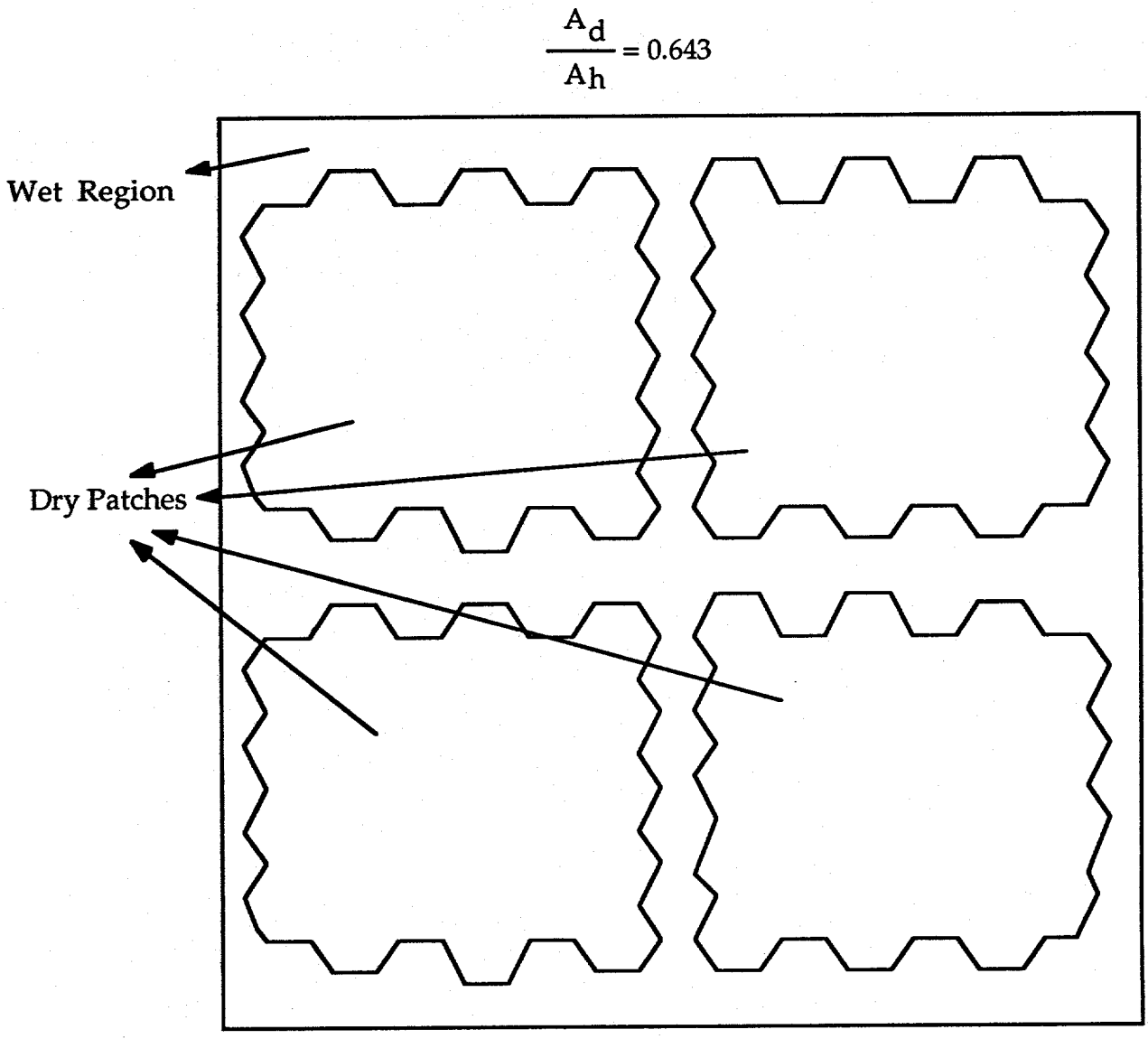

Fig. 11. Sketch of four possible multiple patches on the heater surface.

Table I. Effect of Dry-Patch Shape (Single Patch) on Calculated Values of Hot-Spot Temperatures

Run No.	A_d/A_h	Grid Structure	a (mm)	b/a	STA ΔT (°C)	$\Delta T_{hot\text{-}spot}$ (°C)
1	0.510	irregular	18.10	1.00	43.4	83.0
2	0.490	irregular	14.96	1.47	42.9	81.3
3	0.488	hex	17.82	1.00	43.4	83.3
4	0.488	hex	11.92	2.23	42.2	76.7
5	0.417	hex	16.47	1.00	38.0	76.5
6	0.417	hex	12.45	1.75	37.3	73.0
7	0.417	hex	9.985	2.72	36.2	66.5
8	0.410	irregular	16.40	1.00	37.8	76.3
9	0.410	irregular	13.50	1.48	37.2	74.6
10	0.400	irregular	10.75	2.23	35.3	68.4
11	0.345	hex	14.98	1.00	33.3	68.8
12	0.345	hex	11.56	1.68	32.9	67.0
13	0.345	hex	10.17	2.17	31.8	63.4
14	0.345	hex	9.080	2.72	31.4	59.4
15	0.339	irregular	14.90	1.00	33.1	68.9
16	0.335	irregular	10.85	1.89	32.1	65.3
17	0.334	irregular	8.950	2.69	30.7	60.3
18	0.286	hex	13.64	1.00	30.1	63.4
19	0.286	hex	8.860	2.37	28.7	57.3
20	0.286	hex	6.835	3.98	28.2	51.7
21	0.248	irregular	12.70	1.00	27.6	58.5
22	0.249	irregular	8.980	2.00	27.6	56.7
23	0.249	irregular	6.800	3.48	26.5	50.8
24	0.226	hex	12.13	1.00	27.0	57.3
25	0.226	hex	7.665	2.50	26.3	53.0
26	0.226	hex	6.705	3.27	25.9	50.3
27	0.226	hex	6.060	4.00	25.6	48.3
28	0.113	hex	8.570	1.00	22.5	45.0
29	0.113	hex	4.950	3.00	22.4	42.2
30	0.113	hex	3.915	4.80	22.1	36.5
31	0.113	hex	2.685	10.2	21.8	34.6
32	0.111	irregular	8.540	1.00	22.6	45.6
33	0.107	irregular	4.100	4.34	22.0	39.3
34	0.109	irregular	1.720	6.00	21.7	37.3
35	0.049	irregular	5.600	1.00	20.9	36.7
36	0.049	irregular	1.210	5.50	20.6	31.5
37	0.046	irregular	3.000	3.33	20.8	33.7
38	0.042	hex	5.225	1.00	20.8	36.2
39	0.042	hex	3.740	1.95	20.7	34.0
40	0.042	hex	1.990	6.9	20.6	30.0
41	0.041	irregular	2.070	7.51	20.5	30.3

Table II. Effect of Spacing between Dry Patches on Calculated Values of Hot-Spot Temperatures

Run No.	b/a	Spacing (No. of Cells)	STA ΔT (°C)	$\Delta T_{hot\text{-}spot}$ (°C)
1	7.8	1	21.5	32.6
2	7.8	2	21.5	31.8
3	7.8	3	21.4	31.5
4	7.8	4	21.4	31.4
5	5.03	1	24.7	40.6
6	5.03	2	24.4	38.7
7	5.03	3	24.3	38.0
8	5.03	4	24.2	37.7
9	3.43	1	28.9	50.3
10	3.43	2	28.3	48.0
11	3.43	3	28.1	47.0
12	3.43	4	28.0	46.5
13	2.87	1	37.0	60.5
14	2.87	2	35.9	56.9
15	2.87	3	35.6	55.4

Table III. The Effect of Number of Patches on the Hot-Spot Temperature

Run No.	# of Patches	Total # of Dry Cells	A_d/A_h	STA ΔT (°C)	$\Delta T_{hot\text{-}spot}$ (°C)
1	1	82	0.488	43.4	83.3
2	3	101	0.601	43.0	67.3
3	4	108	0.643	43.1	62.1
4	5	106	0.631	39.8	56.0
5	9	81	0.482	30.5	43.5